
Pyroclastic flows entering the ocean at the Tar River Valley delta

Pyroclastic Flow Induced Tsunami Captured by Borehole Strainmeter during Massive Dome Collapse at Soufriere Hills Volcano, Montserrat, West Indies: Observations and Theory

Elizabeth Van Boskirk (1), Barry Voight (2), Phillip Watts (3), Christina Widiwijayanti (2), Glen Mattioli (1), Derek Elsworth (2), Dannie Hidayat (2), Alan Linde (4), Peter Malin (5), Jurgen Neuberg (6), Selwyn Sacks (4), Eylon Shalev (5), R. Steven J Sparks (7), Simon R Young (2)

(1) Department of Geosciences, University of Arkansas
(2) Department of Geosciences, Pennsylvania State University
(3) Applied Fluids Engineering, Inc.
(4) Department of Terrestrial Magnetism, Carnegie Institution Washington
(5) Division of Earth and Ocean Sciences, Duke University
(6) School of Earth & Environment Earth Sciences, Leeds University
(7) University of Bristol, Department of Earth Sciences

Abstract

Strainmeters at three Caribbean Andesite Lava Island Precision-Seismo-geodetic Observatory (CALIPSO) borehole sites recorded dilitation offset by 7-12 minutes from the seismic signals leading up to 12/13 July 2003 dome collapse eruption of Soufriere Hills Volcano, Montserrat, West Indies. Pyroclastic flows were observed entering the ocean at the Tar River Valley (TRV) delta at 18:00 local time (LT) 12 July. The eruption occurred 23:30 LT 12 July, with dome collapse consisting of 210 x 10^6 m^3 (DRE). Dilatometers at three sites recorded complex, correlated long period oscillatory wave packets with periods ~250-500 s. The strongest oscillatory signal was at Trants, the site nearest to the TRV delta and the coastline. GEOWAVE was used to model wave initiation and propagation to test that pyroclastic flows and dome collapse into the ocean at the TRV delta stimulated tsunami. These tsunami are hypothesized to be signal the strainmeter is observing. The spectral power simulated ocean waves were compared to observed strain at Trants. Simulated wave heights correlate with observations and demonstrate strainmeter sensitivity to geophysical processes not envisioned in the design of the installation at SHV.

CALIPSO Borehole Sites

Each CALIPSO site is equipped with a three component seismometer (Duke CIW Hz-1kHz), Pinnacle Technologies series-5000 tiltmeter, Ashtech U-Z CGPS receiver with choke ring antenna with SCIGN mount and radome, and single component, very-broad-band Sacks-Evertson dilatometer.

Figure 3. AIRS CGPS site.
July 14, 2003. Note ~11 cm of ash accumulation from the July 12/13 collapse. Schematics of the very-broad-band Sacks-Evertson dilatometer (Mattioli et al., 2002)

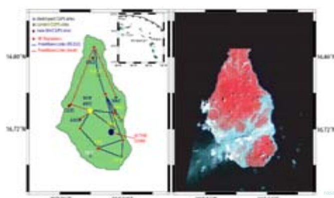

Figure 4. SHV Monitoring Sites
Left: Map of CALIPSO borehole sites (red squares) and other monitoring stations around SHV.
Right: Color Infrared image taken by ASTER. The TRV delta is the grey pyroclastic flow deposits on the eastern side of SHV (Mattioli et al., 2004).

July 12/13 2003 Eruption Timing

The largest dome collapse of Soufriere Hills Volcano removed ~210x10^6 m^3 DRE of material. Several days before the eruption, beginning July 8, increasing seismicity was recorded by small seismic events with the time in between each event decreasing as the eruption approached (Voight et al., 2004). Intense tropical rainfall occurred for two days prior to 12 July.

07:00-09:00 LT 12 July - rainstorm begins and initiates rockfalls and small pyroclastic flows. The pyroclastic flows build in intensity throughout the day.

18:00 LT 12 July - pyroclastic flows are observed reaching the ocean at the Tar River Valley delta, which is ~3km from SHV.

20:00 LT 12 July - pyroclastic surges are observed 2-3 km offshore, suggesting that large volumes of dense units of pyroclastic flows are also entering the ocean. The seismic record shows an increase in pyroclastic flow intensity.

23:00 LT 12 July - peak seismicity occurs during the major dome collapse.

23:34 LT 12 July - transmission from MVO instrument at Whites Yard is lost during dome collapse. Several short volcanian explosions continue resulting from the unroofing of the conduit during dome collapse.

23:39 LT 12 July - HARR seismometer and microphone record the impact of ballistic clasts.

23:45 LT 12 July - GOES-12 satellite observes an eruption cloud at ~16 km.

04:00 LT 13 July - eruption ends with a decreasing seismic signal.

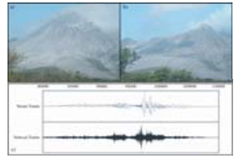

Figure 1. **12/13 July 2003 Eruption**
a) Soufriere Hills Volcano (SHV) taken May 31, 2003. View SSE.
b) Taken August 12, 2003 from the same location. Approximately 210 M m^3 of the dome collapsed during the July 12/13 eruption/dome collapse.
c) July 12-13 2003 dilatometer and vertical seismometer records from TRNT site, which is 5.8 km from SHV. Timescale is in seconds with 0 at July 12 00:44 (Mattioli et al., 2004).

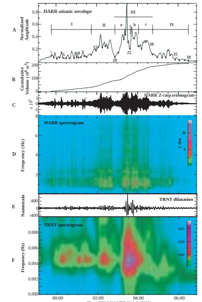

Figure 5. Eruption Seismicity and Dilatation.
A: Normalized seismic amplitude for HARR surface broadband seismometer. All records start at 23:00 (UTC) 12 July 2003. Individual pyroclastic flows are annotated on seismic envelope and major divisions are shown as Roman numerals. B: Cumulative collapse volume from HARR-normalized amplitude in A. C: HARR vertical component seismogram. D: Spectrogram for seismogram in C. Note that most of power is in 1–3 Hz band and that higher frequency energy is observed during significant collapse events. E: TRNT dilatation highpass filtered at >0.002 Hz. Peak amplitudes in dilatation that occur 7–10 min after same events are recorded as seismic energy at HARR. F: Spectrogram for TRNT dilatation in E. Most of power is between 0.004 and 0.006 Hz, and during peak collapse event III, energy is spread to higher frequencies (Mattioli et al., 2006).

GEOWAVE

GEOWAVE uses a Boussinesq model for wave propagation combined with TOPICS, which is input into the program FUNWAVE, to simulate the wave initiation and development of a tsunami (Watts and Waythomas, 2003; Watts et al., 2003; Wei and Kirby, 1995). Detailed bathymetry for the region of Montserrat is smoothed to reenact the underwater pyroclastic flow. The equations to generate a pyroclastic flow are exactly the same used as to generate a wave from a subarial debris flow. GEOWAVE handles frequency dispersion, simulating deep-water waves. The model treats the flow as a solid block that decelerates from an initial velocity. Underwater deformation of the flow is not included in the model (Watts and Waythomas, 2003). GEOWAVE simulated runnup and allows enough entry sources to recreate the geometry of the TRV delta.

Figure 7. Montserrat Bathymetry.
Red stars are CALIPSO borehole sites and TRNT, GERS, and AIRS had operating strainmeters during the eruption. Green circles represent entry sources used in GEOWAVE. The simulated pyroclastic flow has five entry sources to recreate the geometry of the entry at the TRV delta. Blue and orange circles represent gauges used in GEOWAVE. Several gauges (orange) are placed as a radii around Trants and the results are averaged in space for a fixed time. The next step is to calculate the Green's Functions for a load on a uniform elastic half space. We will examine the load over a several km area offshore Trants since the volumetric strain is directly proportional to the dV of the water waves.

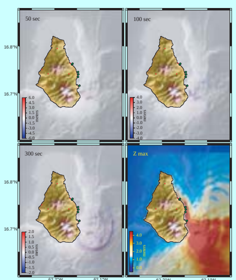

Figure 8. GEOWAVE simulations.
Colors (red for wave heights above and blue for wave heights below sea level) are scaled to model extremes. Simulations are for 7 Mm^3 pyroclastic flow entering sea at ~70 ms–1 with volume to width ratio of 16700 m^2. Z max is maximum wave height over entire temporal domain. Eastern Montserrat, from TRF to Trant's Bay, experienced maximum waves of few meters, with heights as high as 14 m localized proximal to TRF. (Mattioli et al., 2006).

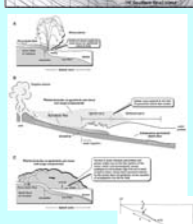

Figure 6a. Cross section of a pyroclastic flow entering the ocean.
Traveling from left to right: a) steam explosion. b) pyroclastic debris flow and plume; c) plume pressure and plume shear. The pyroclastic debris flow would displace water and produce a coherent water wave (Watts and Waythomas, 2003).

Figure 6b. GEOWAVE block model.
Schematics of forces and kinematics of GEOWAVE block acting as a landslide traveling downslope underwater (Watts et al., 2003).

Figure 2. NASA Satellite image taken 14 July 2003
Guadeloupe, ~70 km to the southeast, several witnesses reported an abrupt rise in water between 23:00 LT 12 July and 1:00 LT 13 July (Pelinovsky et al., 2004), which is consistent with the eruption peak at 23:30 LT 12 July. Nevis is to the northwest and Antigua is to the northeast.

Analysis

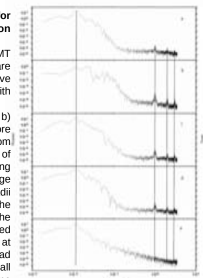

Figure 9. Spectra for GEOWAVE simulation output.
Spectrum1d of GMT was used to compare GEOWAVE wave amplitude outputs with the TRNT dilatation.
a) Spanish Point b) Airport c) Offshore Trants, 250 m from TRNT d) Average of Trants 250 m radii using 5 gauge files e) Average of Trants 500 m radii using 6 gauge files. The lines signify the correlation of increased spectral power at associated with a broad peak at 0.01 Hz in all the synthetic gauge time series.

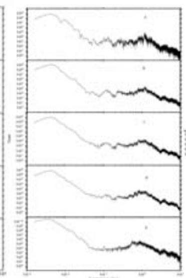

Figure 10. Spectra of TRNT strainmeter.
Unfiltered 12/13 July 2003 eruption data. Each sample of the strain is a sampling of the unobserved signal.

	[illegible]	[illegible]	[illegible]	[illegible]
sample 1	[illegible]	[illegible]	[illegible]	[illegible]
sample 2	[illegible]	[illegible]	[illegible]	[illegible]
sample 3	[illegible]	[illegible]	[illegible]	[illegible]
sample 4	[illegible]	[illegible]	[illegible]	[illegible]
sample 5	[illegible]	[illegible]	[illegible]	[illegible]

Table 1. Strainmeter data was sampled at different wave packets throughout the eruption.
1 b) sample 2 c) sample 3 d) sample 4 e) sample 5.

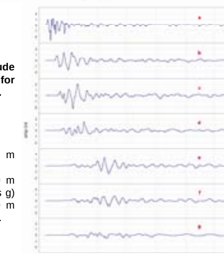

Figure 11. Wave amplitude height in time for GEOWAVE simulation.
a) Entry at Tar River
b) White's Bottom Ghaut
c) Spanish Point
d) Airport
e) Offshore Trants, 250 m from TRNT
f) Average of Trants 250 m radii using 5 gauge files g) Average of Trants 500 m radii using 6 gauge files.

Sensitivity Test Results

The GEOWAVE simulation entry parameters that significantly affect the shoreline wave amplitudes are:

- •final depth and runout length
- •runout time
- •landslide volume
- •runout time

In all cases, the values for the sources of the edge waves (S1 and S2) cause changes in the gauge maximum wave amplitudes.

Conclusions

GEOWAVE, along with the methods applied by Voight and Watts provide parameter limitations to simulate a pyroclastic flow entering the TRV delta in which to create tsunami similar to the 12/13 July 2003 dome collapse and pyroclastic flow events leading up to the peak collapse. Detailed simulations confirm that the unique strainmeter observations may be explained by ocean loading from pyroclastic flow generated tsunami (Mattioli et al., 2006). To quantitatively compare the signals of the strainmeter to the simulated tsunami, however, one needs to solve Green's function, which determines the energy transfer for an elastic half-plane. Also, to further recreate the actual collapse events of 12/13 July 2003, multiple pyroclastic flows causing ocean excitation should be simulated.

Acknowledgements

We thank the CD and IF programs at NSF-EAR and the UK NERC for support. UARK, CIW, and PSU provided significant cost-shares. MVO staff aided installation and initial operation phases of CALIPSO. Students from our institutions and the University of the West Indies made valuable contributions during drilling and installation.

References

Hidayat, D., Linde, A., G.S. Mattioli, S.R. Young, B. Voight, S.J. Sparks, E. Shalev, S. Sacks, P. Malin, W. Johnston, D. Elsworth, P. Dunkley, R. Herd, J. Neuberg, G. Norton, and C. Widiwijayanti (2004), unpublished

Linde, A., G.S. Mattioli, S.R. Young, B. Voight, S.J. Sparks, E. Shalev, S. Sacks, P. Malin, W. Johnston, D. Hidayat, D. Elsworth, P. Dunkley, R. Herd, J. Neuberg, G. Norton, and C. Widiwijayanti (2004), unpublished.

Mattioli, G., D. Elsworth, A. Linde, P. Malin, N. McWhorter, D. Nielson, S. Sacks, E. Shalev, B. Voight, and S. Young, 2002, Magma reservoir and conduit dynamics as revealed by a borehole geophysical observatory and continuous GPS: The CALIPSO Project plan and goals, EarthScope Workshop on Active Magmatic Systems (Nov. 2002), Heathman, WA

Mattioli, G.S., A.T. Linde, I. S. Sacks, P. Watts, C. Widiwijayanti, S..R Young, B. Voight, D. Hidayat, D. Elsworth, P.E. Malin, E. Shalev, E. Van Boskirk, W. Johnston, R.S.J. Sparks, J. Neuberg, V. Bass, P. Dunkley, R. Herd, T. Syers, P. Williams, and D. Williams, 2006, Unique and remarkable strainmeter measurements of pyroclastic flow-generated tsunami, *Geology*, **in press**.

Mattioli, G.S., S.R. Young, B. Voight, R.S.J. Sparks, E. Shalev, S. Sacks, P. Malin, A. Linde, W. Johnston, D. Hidayat, D. Elsworth, P. Dunkley, R. Herd, G. Norton, J. Neuberg, and C. Widiwijayanti, 2004, Prototype PBO Instrumentation of CALIPSO Captures World-Record Lava Dome Collapse of July 2003 on Soufrière Hills Volcano, Montserrat (Feature article), *EOS transactions, American Geophysical Union*, **85**, 317-328.

Mattioli, G.S., B. Voight, A.T. Linde, I.S. Sacks, P.Watts, C. Widiwijayanti, S.R. Young, D. Hidayat. D. Elsworth, P.E. Malin, E. Shalev, E. Van Boskirk, W. Johnston, R.S.J. Sparks, J. Neuberg, V. Bass, P. Dunkley, R. Herd, T. Syers, P. Williams, and D. Williams (2006), Unique and Remarkable Dilatometer Measurements of Pyroclastic Flow-Generated Tsunami Waves, Geology.

Van Boskirk, E., 2006, Pyroclastic Flow Generated Tsunami Recorded by CALIPSO Borehole Strainmeters at Soufreiere Hills Volcano, Montserrat During Massive Dome Collapse, Masters Thesis, University of Arkansas.

Voight, B., G.S. Mattioli, S.R. Young, S.J. Sparks, E. Shalev, S. Sacks, P. Malin, W. Johnston, D. Hidayat, D. Elsworth, P. Dunkley, R. Herd, J. Neuberg, G. Norton, and C. Widiwijayanti (2004), Capture of World-Record Lava-Dome Collapse on Montserrat by CALIPSO Borehole Instrumentation Project, draft manuscript for submission.

Walder, J.S., P. Watts, O.E. Sorenson, and K. Janssen (2003), Tsunami generated by subarial mass flows, *Journal of Geophysical Research*, 108(B5), 2236.

Watts P., C.F. Waythomas (2003), Theoretical analysis of tsunami generation by pyroclastic flows, *Journal of Geophysical Research*, 108(B12), 2563.

Watts, P., Grilli, S.T., Kirby, J.T., Fryer, G.J., and Tappin, D.R., 2003, Landslide tsunami case studies using a Boussinesq model and a fully nonlinear tsunami generation model: Natural Hazards and Earth System Sciences, v. 3, p. 391-402.

Wei, G., and Kirby, J.T., 1995, Time-dependent numerical code for extended Boussinesq equations: Journal of Waterway, Port, Coastal and Ocean Engineering, v. 121, p. 251-261.